ISSN 1063-7842, Technical Physics, 2022, Vol. 67, No. 5, pp. 411–422. © Pleiades Publishing, Ltd., 2022.
ISSN 1063-7842, Technical Physics, 2022. © Pleiades Publishing, Ltd., 2022.
Russian Text © The Author(s), 2021, published in Zhurnal Tekhnicheskoi Fiziki, 2021, Vol. 91, No. 10, pp. 1479–1490.

Anodic Alumina Prepared in Aqueous Solutions of Chelating Complex Zinc and Cobalt Compounds

A. A. Poznyak[a,*], G. H. Knörnschild[b], A. N. Pligovka[a], and T. D. Larin[a]

[a] *Belarusian State University of Informatics and Radioelectronics, Minsk, 220013 Belarus*

[b] *Universidade Federal do Rio Grande do Sul, 91501970 Porto Alegre, Brazil*

**e-mail: poznyak@bsuir.by*

Received April 15, 2021; revised April 15, 2021; accepted April 15, 2021

Abstract—Results of galvanostatic anodic oxiding of specially prepared high-purity aluminum in aqueous solutions of complex compounds $K_3[Co(C_2O_4)_3]$ and $K_2[Zn(edta)]$ with different concentrations in the current-density ranges of, respectively, $(1.5–1.10) \times 10^2$ and 1.5–30 mA cm^{-2} are presented. Kinetic features of anodic oxiding indicating the presence of an oscillating electrochemical process are established. The following morphological features atypical of anodic alumina are revealed: "flaky and loose" formations for $K_2[Zn(edta)]$ and "monolithic" formations for $K_3[Co(C_2O_4)_3]$. The elemental composition and IR spectroscopic and photoluminescence characteristics of the formed oxides are presented.

Keywords: anodic alumina, chelating complex compounds, anodic oxiding

DOI: 10.1134/S106378422206007X

INTRODUCTION

A promising line of research in nanotechnologies, which is currently being intensely developed, is the formation of nanostructures and composite materials using porous anodic alumina (AA) as a highly ordered nanostructured matrix [1–3]. The cellular-porous structure of AA opens wide possibilities for controlling its morphological parameters and makes it possible to design various functional materials [4–10].

Electrolyte composition plays an important role in the structure formation of anodic oxides of valve metals (titanium, hafnium, niobium, tantalum, tungsten, vanadium, and zirconium) [11–14]. It should be noted that the formation of porous and tube oxides of these metals became possible due to the addition of small amounts of fluoride ions to the anodic oxiding electrolytes; these ions are ligands that form strong complex compounds with many metal ions [15]. The composition of the electrolyte of aluminum anodic oxiding [16–18] and experimental conditions [18–20] also significantly affect the properties and composition of AA. The processes of AA formation in electrolytes, which contain complex compounds and/or ligands capable of forming stable complex compounds, are of great interest from the point of view of additional possibilities for controlling the AA composition [21].

The idea of introducing complexing additives into electrolytes for cathodic deposition of coatings is not new; it has been used in practice for a long time [22, 23]. Processes related to ac or cathode coloring of previously formed AA layers often imply the presence of complexing organic reagents as well [24]. The process of AA modification, which consists in cathodic deposition of indium antimonide into AA pores, also implies a high concentration of citrate anions [3].

It should be noted that some acids used for preparation of anodic oxiding electrolytes [25–28] have a pronounced tendency to the formation of soluble complex compounds with aluminum ion [15]. As was shown previously [18], one can intentionally add materials containing ligands that form stable soluble complex compounds with aluminum [15], which changes significantly both the character of anodic oxiding process and the AA morphology. Similar studies were performed using the organic reagent arsenazo I (disodium salt of 3-[(2-arsonophenyl)azo]-4,5-dihydroxy-2,7-naphthalenedisulfonic acid), which forms extremely stable chelating complexes with Al^{3+} and some other ions [15]. The first brief communication on this subject appeared as early as in 2003 [29]; then the research was continued and its results were presented in a series of short papers [30–35]. It was shown in those studies that an increase in arsenazo I concentration leads to a stepwise increase in the dissolution rate and a decrease in values of the maximum and steady-state voltages of the anodic-oxiding kinetics; the threshold additive concentration tends to increase with an increase in the anodic current density and the "burning" phenomenon, described, e.g., in [36–38], disappears. It was reported in [31, 32, 39] that an anomalously high con-

tent of electrolyte components incorporated into the AA structure during its formation was achieved for the first time.

One can also introduce additives that form stable complex compounds insoluble in an electrolyte (for example, o-hydroxyquinoline and/or its derivatives) [15]. Anodic oxiding in electrolytes with such additives leads to the improvement of electrical characteristics of the formed AA [40] and a change in its spectral-luminescent properties [39].

Along with the introduction of additives of materials, which contain ligands capable of forming soluble or insoluble complex compounds with ions of the anodized valve metal, into the anodic oxiding electrolyte, one can use an approach in which the additive is a beforehand synthesized stable complex compound containing ions of a complexing agent of a different nature (rather than ions of the anodized metal). To the best of our knowledge, there are only a few studies on this subject [39, 41, 42].

In the works devoted to anodic oxiding in solutions of zinc and cobalt complex compounds [39, 41], the authors mentioned the phenomenon of periodic voltage oscillation and discovered an unusual AA surface morphology. It was shown in a study on anodic oxiding in the presence of chelating complex compounds of copper that the amount of copper incorporated into alumina walls increases with an increase in the oxide growth rate (i.e., voltage and temperature), which deteriorates the regularity of nanopore arrangement. Investigation of the photoluminescence (PL) confirmed the inclusion of chelating copper complexes [42].

Reproducible and targeted control of not only morphology but also composition of AA is an urgent problem of technical physics and materials science; solution of this problem would allow one to form AA materials with specified electrical characteristics and morphology and dope oxide cell walls to provide conducting, semiconductor, or peculiar optical properties, which, in turn, expands the range of AA application. One way to the change electrical and/or optical characteristics of AA is anodic oxiding in complexing solutions or solutions, containing complex compounds of various metals. Although this technique has been approved in practice [40], it has not been thoroughly investigated: there are only a few publications in the form of conference theses and even fewer papers. The above-described studies do not comprise complete and specific concept about the process of AA formation in electrolytes with additives or based on complex compounds; their results should be complemented and refined. The purpose of this study was to supplement the results of the previous studies, investigate more thoroughly the process of anodic oxiding in aqueous solutions of chelating complex compounds of zinc and cobalt, to characterize the formed AA, and to present new data for making a general picture of the process of anodic oxiding under aforementioned conditions.

1. EXPERIMENTAL

1.1. Preparation of Aluminum for Anodic Oxiding

In this study, Al (99.999%) and chemical agents produced by Aldrich Chemical Co were used. The aluminum thickness was 1 mm. For realization of subsequent anodic oxiding, aluminum sheets were cut into samples with a necessary size so as to make the anodized area be about 1 cm^2. To remove internal stress and reduce the number of dislocations [43, 44], the samples after the cutting were subjected to thermal treatment. The samples were first annealed at a temperature of 753 K for 1 h and then cooled in room-temperature water.

After annealing, the samples were subjected to mechanical treatment, which consisted in successive grinding and polishing of a metal surface from both sides. The samples were first ground using a MicroCut special grinding paper for wet grinding with SiC-based abrasive (granularity 1200 in accordance with the ANSI standard); afterwards, they were subjected to successive polishing on polishing wheels with application of diamond pastes (grain size 3 μm) and finishing with an abrasive OPS suspension based on aluminum oxide. The surface quality after the treatment corresponded to the 14th-grade finish.

In view of the relatively high cost of the materials, many of the samples were used two to three times; in this case, they were subjected again to thermal treatment and, then, to grinding and polishing according to the aforementioned technique. It is reasonable that their thickness decreased to 0.3–0.7 mm, in dependence of the number of cycles. It is assumed that the composition and properties of these samples did not change.

Before the anodic oxiding, the meniscus region was shielded with a barrier oxide, formed in 1% citric acid (the structural formula is shown in Fig. 1a) in a combined regime. First, the voltage was swept with a rate of 2.0 V/s in the potentiodynamic mode; after reaching 290 V, the mode changed to potentiostatic, and the anodic oxiding was stopped when the current became about 1% of the initial value. The anodic oxiding was carried out in the galvanostatic (GS) mode (j_a = const) in a glass electrochemical cell with a planar platinum cathode, the area of which is comparable to that of the anode; the anode and cathode were arranged vertically and mutually parallel (one side of the anodized sample faced the cathode, while the other side was directed oppositely).

1.2. Anodic Oxiding Electrolytes

Anodic oxiding electrolytes were aqueous solutions of Co(III) and Zn(II) complex compounds, synthe-

sized according to the below-described techniques. The techniques of preparation of solutions of cobalt and zinc complex compounds are identical in principle. First, hydroxide of a corresponding metal was precipitated from an aqueous solution of its sulfate by adding a potassium hydroxide solution to the sulfate solution in an equivalent amount (Eq. (1)). Sulfates were preferred (e.g., in comparison with chlorides) primarily because small amounts of impurities of chloride ions, which may be present in the synthesized compounds even after their thorough purification, would make further implementation of the anodic oxiding of aluminum and/or its alloys impossible because of pitting [45]. The precipitating agent was chosen to be potassium hydroxide (rather than, e.g., sodium hydroxide), because a sodium ion is known to be characterized by fairly high mobility, which makes its presence undesirable in technological processes of production of the element base of microelectronic devices.

The precipitate was drawn off through a dense paper filter using a water-jet pump and washed several times with distilled water. To prepare the ethylenediaminetetraacetate complex (Eq. (2)), the precipitate on the filter paper was placed in the beforehand prepared solution of dipotassium salt of ethylenediaminetetraacetic acid (the structural formula is presented in Fig. 1b). The metal hydroxide was dissolved under intense stirring. All reactions were performed as fast as possible at room temperature (without heating) to prevent decomposition of unstable hydroxides due to water detachment (Eq. (3)), which would, in turn, hinder the run of the complexing reaction.

$$ZnSO_4 + 2KOH \rightarrow Zn(OH)_2\downarrow + K_2SO_4, \quad (1)$$

$$Zn(OH)_2 + K_2H_2edta \rightarrow K_2[Zn(edta)] + 2H_2O, \quad (2)$$

$$Zn(OH)_2 \rightarrow ZnO + H_2O. \quad (3)$$

The solutions were then filtered and, after corresponding dilution, used for anodic oxiding. The complex cobalt compound $K_3[Co(C_2O_4)_3]$ (the coordination number of cobalt in the oxidation state of +2 and +3 is generally equal to 6) was synthesized in a similar way, with the only difference being that oxalic acid was used instead of K_2H_2edta (Fig. 1c).

1.3. Instruments and Equipment

The composition of the obtained experimental samples was studied by X-ray photoelectron spectroscopy (XPS) on a Physical Electronics PHI 5600XP spectrometer, IR spectroscopy with the spectral resolution of 1 cm^{-1} using a Perkin-Elmer-180 and Auger electron spectroscopy on a Physical Electronics PHI 670 device. Electron microscopy studies were carried out using JEOL JSM 6400 and Hitachi S4800 scanning electron microscopes equipped with a Genesis 4000 electron-probe attachment. Optical

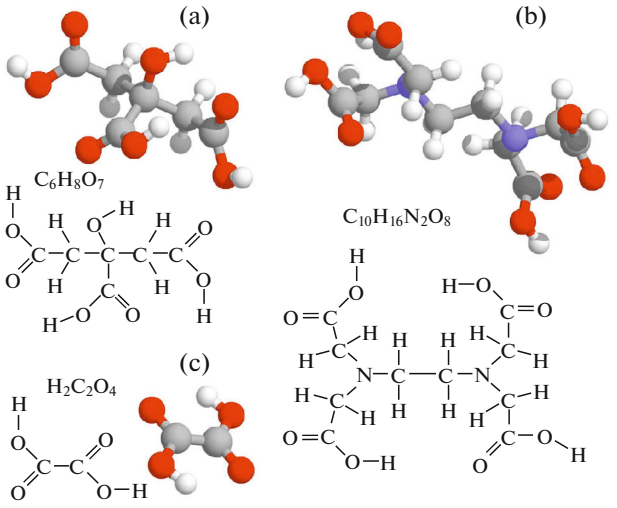

Fig. 1. Structural formulas and 3D models of organic-acid molecules: (a) citric acid, (b) ethylenediaminetetraacetic acid, and (c) oxalic acid.

images were obtained on a Micro 200-01 microscope. Photoluminescence spectra were obtained using an SFL-1211 A spectrofluorimeter at a spectrometer slit width of 1 nm. X-ray-diffraction spectra were recorded on an upgraded DRON-3 system (CuK_α radiation, graphite filter) at the scanning step of 0.04° and exposure for 3 s at each point in the 2θ range of 15°–100°.

2. RESULTS AND DISCUSSION

In the case of aluminum anodic oxiding in an electrolyte, which is an aqueous solution of the complex compound $K_2[Co(edta)]$ (0.75 M, 1.5 mA cm^{-2}), one can observe a pronounced "burning" phenomenon characterized by oscillations of the anodic voltage in kinetics, despite the intense stirring and low anodic current densities; this phenomenon was described in [46]. Typical kinetics of the anodic process in this electrolyte is shown in Fig. 2a. A completely different situation was observed for anodic oxiding of high-purity aluminum samples in the $K_2[Zn(edta)]$ solution [41]. The complex salt concentration was 0.5 M in all cases, and anodic current density j_a was varied in the range of 1.5–30 mA cm^{-2}. The anodic-oxiding kinetics (time dependence of anodic voltage U_a) of one of the samples is shown in Fig. 2b.

The anodic process running in the $K_2[Zn(edta)]$ solution has a number of significant kinetic features. In the beginning, as in acid electrolytes, one observes an almost linear increase in the anodic voltage with time to a maximum value; afterwards, the voltage somewhat decreases and, then, instead of transition to the stationary mode, there is a significant, gradually slowing down increase in the anodic voltage. After

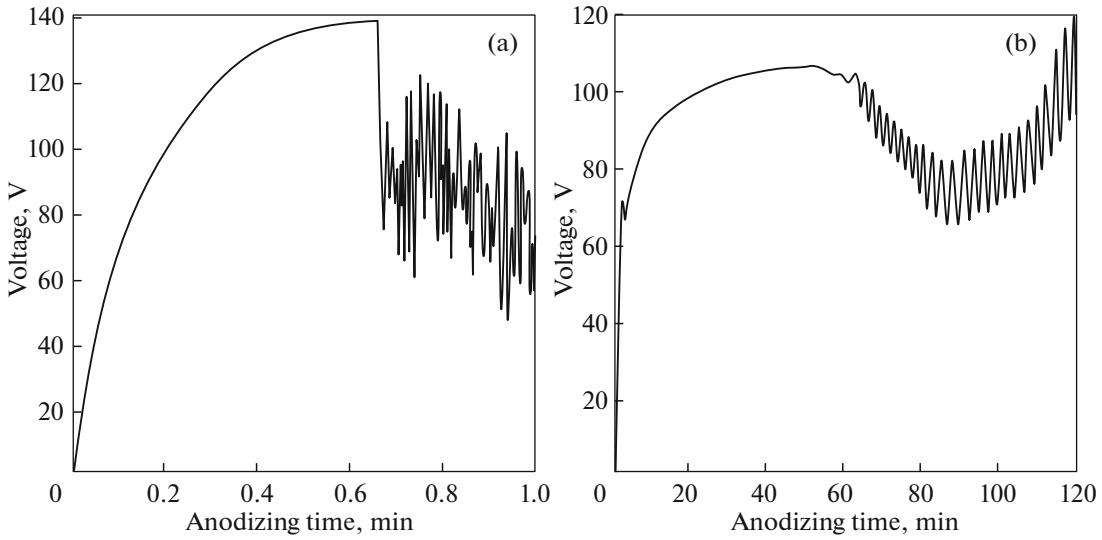

Fig. 2. Kinetics of Al anodic oxiding in (a) 0.75 M aqueous solution of Co *edta* complex at the current density j_a of 1.5 mA cm^{-2} and (b) 0.5 M aqueous solution of K_2[Zn(*edta*)] at current density j_a of 5 mA cm^{-2}.

several tens of minutes, when the U_a value almost ceases to grow, periodic voltage oscillations occur. The U_a value is as high as ~100 V at the maximum, and the oscillation amplitude is up to 20 V. Oscillations do not disappear at the anodic oxiding duration up to 120 min. This phenomenon should be considered separately. To date, a large number of oscillating chemical reactions are known [47]; the first phenomena related to oscillation behavior of electrochemical systems were discovered in the early 20th century [48]. Ever since, a great amount of experimental results on self-organization phenomena occurring during electrode processes have been accumulated. Until recently, four groups of oscillating electrochemical reactions have been known [48]. These oscillations occur in some cases at

(i) anodic dissolution of metals;

(ii) anodic oxiding of nonmetallic materials (mainly, organic compounds and hydrogen);

(iii) cathodic deposition of metals; and

(iv) electroreduction of anions.

It can be seen that periodic reactions running during anodic passivation have not been observed yet. Therefore, comprehensive investigation of the obtained films is of particular interest.

Figures 3a–3c show electron-microscopy images of the surfaces of the samples subjected to anodic oxiding in 0.5 M solution of K_2[Zn(*edta*)] at different j_a values. It can be seen that, even at a low current density (1.5 mA cm^{-2}) and 30-min duration of anodic oxiding, protrusions are formed on the surface, which merge into continuous crack fields with an increase in the current density to 4.0 mA cm^{-2} and that of the process duration to 2 h. A further increase in j_a (to 10.0 mA cm^{-2}) at anodic oxiding for 20 min leads to the formation of "flaky" (or "loose") protrusions, the sizes and surface density of which increase with a further increase in the process duration and the current density (to 25 mA cm^{-2}). A high-magnification electron-microscopy image of a crack is presented in Fig. 3d. It can be seen that AA has a cellular-porous structure at crack kink. The formations shown in Fig. 3 are visually similar to the objects presented in SEM images of previous studies on anodic oxiding aluminum in different acids [49–51] and the recent work [20], as well as to microcones growing at anodic oxiding of titanium [52, 53]. This circumstance may be indicative of a common character of the reasons inducing these formations. Apparently, there is a local redistribution (ordered, to some extent) of the current density and the concentration of different-nature ions, which may lead both to the growth of more or less regularly located of microprotrusions [20, 52, 53] and the formation of randomly located breakdowns [49–51].

The occurrence of "smooth" (at small j_a values) and "flaky" protrusions (at a further increase in the anodic current density) can be explained by the fact that small impurity anions, present in the solution in trace amounts, are concentrated near certain surface portions due to the current density redistribution and cause local nonuniform conductivity of the electrolyte. In addition, impurities can be incorporated into AA both homogeneously over the entire area and inhomogeneously [16]. In the latter case, an oxide portion with a larger number of anions has a higher conductivity, which leads to an increase in its growth rate. In our case, the relief inhomogeneity at anodic oxiding arises in the complex compound solutions under the study in a similar way.

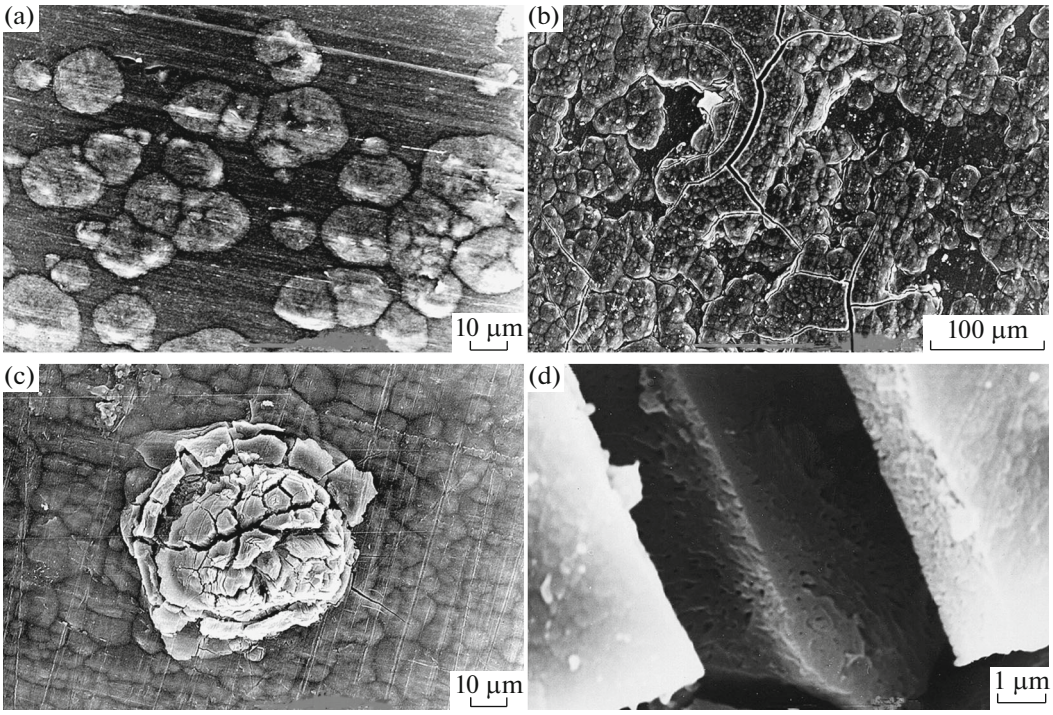

Fig. 3. (a–c) Micrographs of the AA surfaces formed in the (a, b) 0.5 M solution of K_2[Zn(*edta*)] at j_a = (a) 1.5, (b) 4.0, and (c) 10.0 mA cm^{-2} for 30 min, 2 h, and 20 min, respectively, and a crack on the AA surface, formed at the current density of 14.0 mA cm^{-2} for 2.5 h.

In this study, we also performed analysis of AA films obtained by electrochemical GS anodic oxiding of aluminum in the K_2[Zn(*edta*)] solution using the electron-probe, Auger-spectroscopy, and XPS methods. For the case of dielectric materials (in particular, Al_2O_3), the XPS analysis involves some difficulties in the interpretation of the obtained spectra [54]. Such analysis implies charge accumulation on samples; therefore, the peak positions should be corrected with respect to the Auger peak of oxygen, which allows one to determine the electron binding energy and the valence state of elements. The Auger-electron and XPS analyses showed the presence of carbon, nitrogen, and sulfur impurities in the AA composition. Figure 4 shows the results of analyzing a "loose" protrusion of the sample, obtained by anodic oxiding for 55 min at the anodic current density of 25 mA cm^{-2} after conventional (Fig. 4a) and long-term (Fig. 4b) washing; the results of analyzing the state of some elements, entering into the composition of the same object, are presented in Figs. 4c–4e.

The samples were washed in room-temperature distilled water under continuous stirring in a volume of ~100 mL with the washing water changed three times; the total washing duration was ~15 min. The repeated analysis was performed after fivefold washing under the same conditions but at the total duration of about 5 h. As follows from the analysis results, sulfur (presumably, as sulfate anion) enters into the composition of the oxide rather than being sorbed by the loose structure of the protruding formation on the surface, because it was not removed after the long-term washing. The analysis of the valence state of elements showed that alumina is in the form of α or γ modification (this method cannot ensure more accurate identification), carbon is bound by the nonpolar or weakly polar bond (of the C–C, C–H, or C–S type), and sulfur is present in the oxidized state (i.e., it is indeed in the form of sulfate anion). The presence of sulfur is most likely explained by contamination of the synthesized complex compound with potassium sulfate; despite the trace concentration of sulfate anion in the electrolyte, it is more efficiently incorporated into the formed oxide because of a small ionic radius and a higher mobility. Carbon could be brought into the AA film only along with the acid residue of *edta*. The latter statement is favored by the presence of nitrogen impurity in the oxide, which also enters into the composition of ethylenediamine–tetraacetic acid. The analysis did not exhibit a signal from highly polar C=O and C–O bonds because, first, the fraction of these atoms in $edta^{4-}$ anion is small (in comparison with the number of atoms bound by a weakly polar or nonpolar bond) and, second, the total amount of carbon in the film is insignificant. However, the reported analysis results indirectly indicate the presence of zinc in the composition of obtained AA, which cannot but be

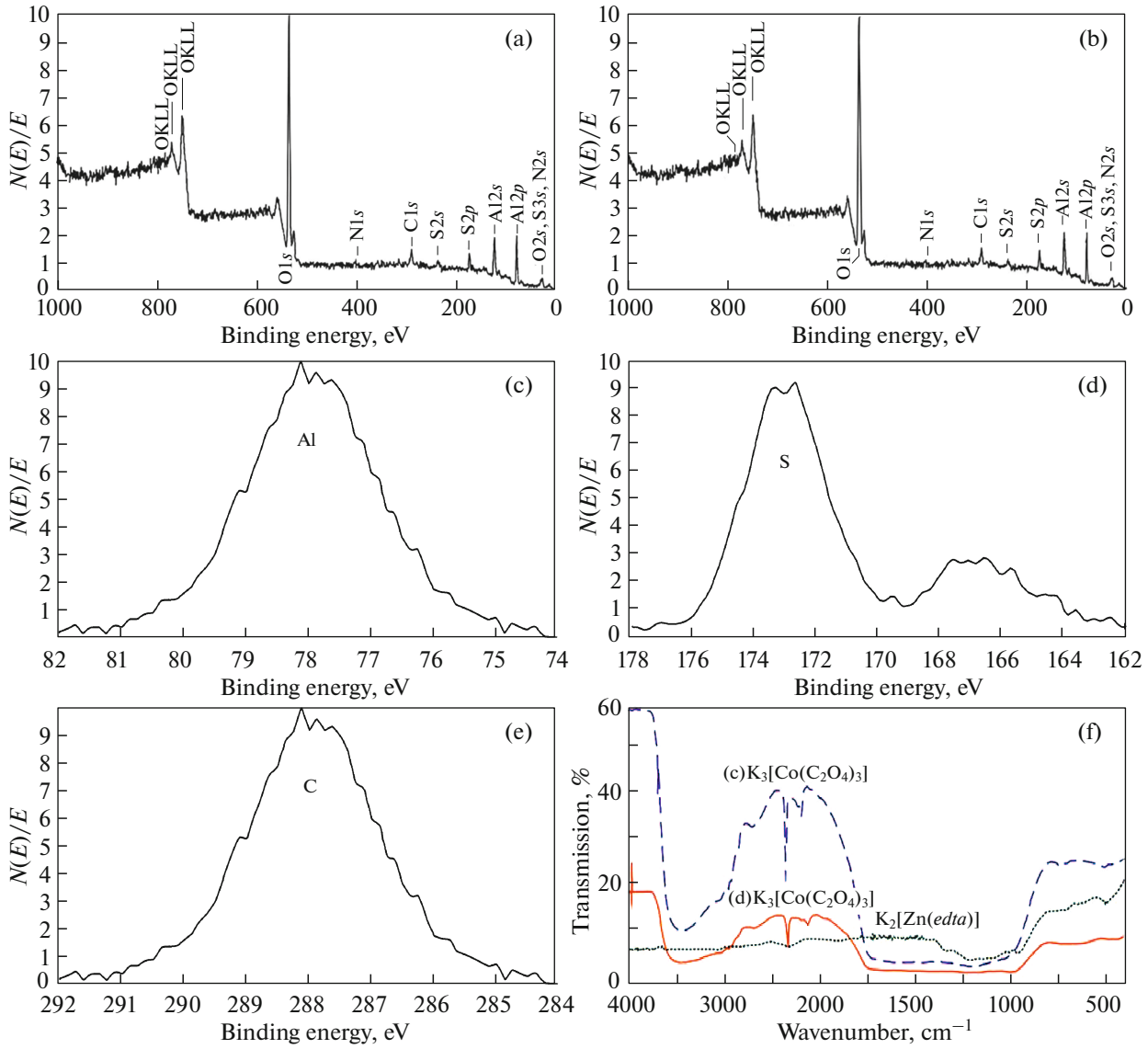

Fig. 4. (a, b) XPS data for a "loose" protrusion of the sample obtained by anodic oxiding for 55 min at the anodic current density of 25 mA cm^{-2} after (a) conventional and (b) long-term washing. (c–e) XPS identification of the valence state of (c) aluminum, (d) sulfur, and (e) carbon in the composition of the "loose" protrusion; and (f) IR transmission spectra of the sample formed in the 0.5 M solution of K_2[Zn(*edta*)] for 55 min at the anodic current density of 25 mA cm^{-2} and the samples shown in Figs. 6c and 6d.

brought into the film in the composition of extremely strong complex chelating ethylenediaminetetraacetate doubly charged anion [Zn(*edta*)]$^{2-}$ [15]. Indeed, zinc impurities were also found in the oxide composition by the electron-probe analysis. The amount of each impurity element does not exceed ~1 at %. The impurities are caused by penetration of the electrolyte components into the AA structure.

Figure 5a shows the PL spectra of AA obtained by anodic oxiding in the K_2[Zn(*edta*)] solution for 55 min at an anodic current density of 25 mA cm^{-2} and excitation wavelengths of 260 and 340 nm. It can be seen that, at the above λ_{ex} values, the PL spectra of this sample barely differ from those of the samples obtained in conventional acid electrolytes. At the same time, the sample absorbs very strongly not only in the visible region, but also in the IR range. Figure 4f shows the IR transmission spectrum of the same sample in a wide range of wave numbers. Even in the longest-wavelength range (800–400 cm^{-1}), the region of the highest transparency of this sample), the relative transmittance hardly reaches 20%. Because of the extremely high absorption and indistinct transmission minima, the analysis and interpretation of the spectrum are difficult even at a high sensitivity of an IR spectrometer.

A series of experiments on anodic oxiding of high-purity aluminum samples in the GS mode in the solu-

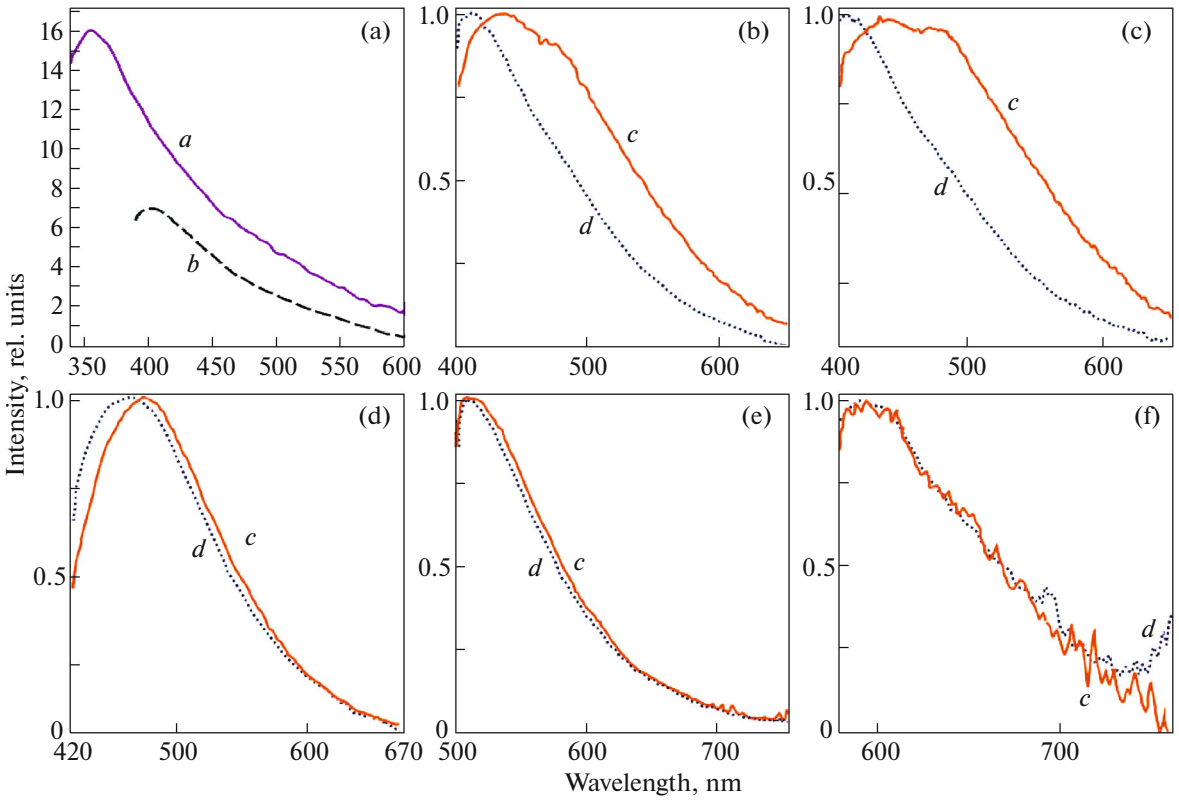

Fig. 5. PL spectra of the AA sample obtained in the (a) 0.5 M solution of $K_2[Zn(edta)]$ for 55 min at the anodic current density of 25 mA cm^{-2} (solid line *a* and dashed line *b* correspond to the excitation wavelengths of 260 and 340 nm, respectively) and (b–f) 1.9 M solution of $K_3[Co(C_2O_4)_3]$ for 29 min at $j_a = 1.10 \times 10^2$ mA cm^{-2} at excitation wavelengths of (b) 270, (c) 308, (d) 370, (e) 415, and (f) 520 nm (solid lines *c* and dotted lines *d* correspond to the surface faced the cathode (Fig. 6c) and the opposite surface (Fig. 6d), respectively).

tion of oxalate chelating cobalt complex $K_3[Co(C_2O_4)_3]$ was performed. The electrolyte concentration in the experiments was 1.1 and 1.9 M, and the current density ranged from 1.5 to 1.10×10^2 mA cm^{-2}. The anodic-oxiding kinetics is similar on the whole to that described for the case of ethylenediaminetetraacetate complex of zinc, with the following differences: first, the anodic voltage at the maximum hardly reached 100 V, and, second, the oscillation frequency was higher and oscillation amplitude was ~1 V.

Figures 6a and 6b show electron- and optical-microscopy images of the surface of AA formed by anodic oxiding of Al for 74 min in the 1.9 M solution of $K_3[Co(C_2O_4)_3]$ at the current density of 50.0 mA cm^{-2}. Since the electron microscope has a higher resolution and depth of focus [55], its image exhibits more clearly the character of the sample surface, whereas the optical image demonstrates the color of the formed AA. It can be seen that protruding formations with a conical or quadrangular-pyramid shape are located on the relatively flat AA surface; under certain conditions, these formations merge to form continuous fields. The character and total area of these formations depend on the electrical regime of anodic oxiding and the orientation of the anodized sample with respect to the cathode. Figure 6 show optical photographs of the AA, obtained by anodic oxiding in the 1.9 M solution of $K_3[Co(C_2O_4)_3]$ for 29 min at $j_a = 1.10 \times 10^2$ mA cm^{-2} (the side facing the cathode (Fig. 6c) and the opposite side (Fig. 6d)). The samples obtained at higher anodic current densities are characterized by a larger number of formations with a larger size (especially at the side facing the cathode); they exhibit no cracking and "peeling" at any current density. In other words, the oxide thickness on the anodic side facing the cathode is larger than that on the opposite side, which not only follows from the observation of Figs. 6c and 6d, but is also indirectly confirmed by the results of studying the PL and IR spectroscopic properties and the X-ray diffraction data (Fig. 7). This influence is indicative of a low scattering power of the used electrolyte. The term "scattering power" is used to estimate the uniformity of the current distribution on the electrodes, which means the ability of electrolyte to yield more or less uniform coating thicknesses under certain electrolysis conditions [56].

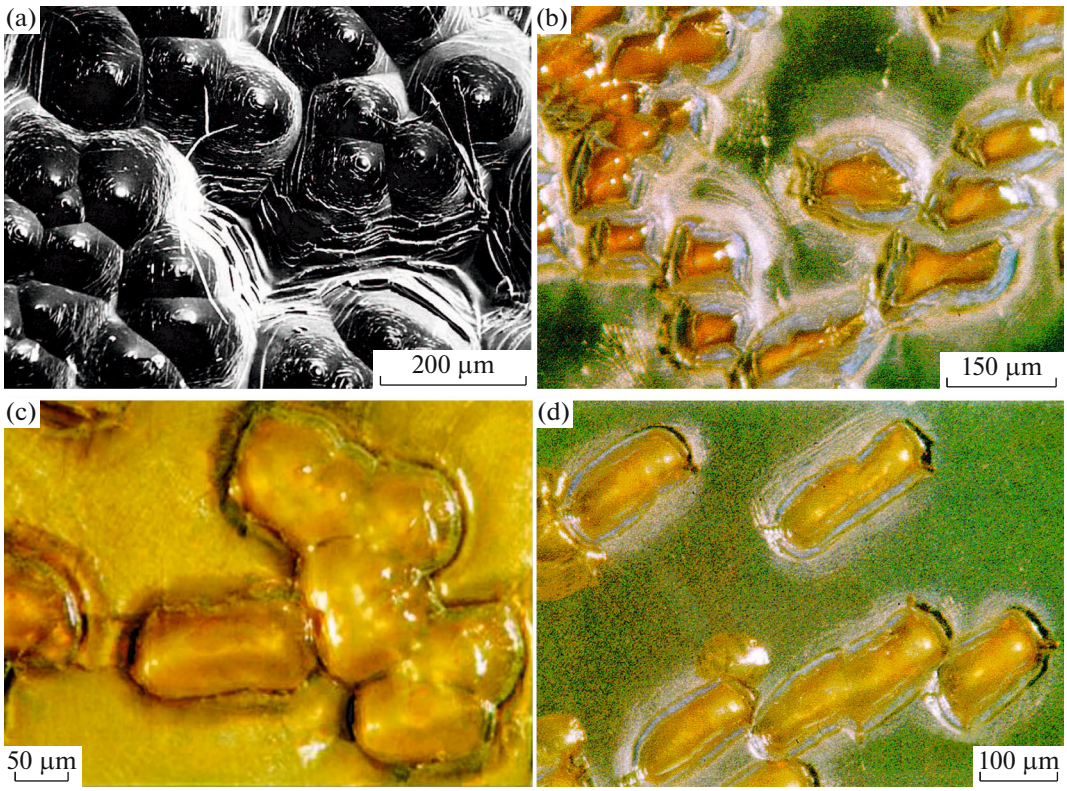

Fig. 6. (a) Electron- and (b) optical-microscopy images of the surface of anodic alumina obtained by anodic oxiding in the 1.9 M solution of $K_3[Co(C_2O_4)_3]$ for 74 min at a current density of 50.0 mA cm^{-2}; (c, d) optical photographs of AA obtained by anodic oxiding in the 1.9 M solution of $K_3[Co(C_2O_4)_3]$ for 29 min at $j_a = 1.10 \times 10^2$ mA cm^{-2} at the (c) side facing the cathode and (d) opposite side.

It was established that the presence of the above-noted protrusions causes significant differences in the PL properties in comparison with other films prepared under similar conditions. Figures 5b–5f present PL spectra of different sides of the same sample (shown in Figs. 6c, 6d), recorded at different excitation wavelengths (λ_{ex} = 270, 308, 370, 415, and 520 nm). Curves *c* in the plots show the AA spectra at the sample side facing the cathode, while curves *d* correspond to the opposite side. All luminescence spectra in Figs. 5b–5f are normalized on unity. The characters of the presented spectra have pronounced differences. First, the spectrum of the surface with many protrusions is significantly red-shifted; second, the occurrence of protrusions on the sample surface gives rise to the pronounced second maximum in the longer-wavelength region (in comparison with the main maximum), which disappears with an increase in the excitation wavelength. Both specific features become more pronounced with a decrease in the excitation light wavelength. This fact indicates that the protrusion composition includes luminescence centers, which are excited by shorter waves. Further investigations should be carried out to determine the nature of these centers and reveal differences in the structure and composition of AA layers with protrusions and without them.

Figure 4f presents IR spectra of the sample obtained by anodic oxiding of aluminum in the $K_3[Co(C_2O_4)_3]$ solution (shown in Figs. 6c, 6d). Curve *c* is the AA spectrum at the sample side facing the cathode, while curve *d* corresponds to the opposite side (both surfaces are presented in Figs. 6c and 6d, respectively). In comparison with similar spectra that are typical of electrolytes containing no additives of complex cobalt compounds, new absorption bands arose. The bands in the regions of 3750–2800 and 2100–800 cm^{-1} are very wide and strong, even at low spectrometer sensitivity. One can also observe weaker but very narrow absorption bands with sharp minima near the wavenumbers of 2350 and 2150 cm^{-1} (the latter is a double band). When trying to resolve these bands, we reduced the device sensitivity so that the generally pronounced wide strong absorption band in the region of 1000–400 cm^{-1}, actually composed of several bands and corresponding to Al–O stretching vibrations, becomes hardly distinguishable.

Problems of the IR spectroscopic analysis of AA obtained in aqueous solutions of sulfuric, orthophos-

phoric, oxalic, and malonic acids were considered in detail in [57]; it was shown that AA formed in these electrolytes has a low (at the spectrophotometer sensitivity limit) degree of hydration and a low boehmite concentration. It is interesting to note the presence of strong absorption bands in the range of 3700–3000 cm^{-1} and near 1060 cm^{-1}, which are indicative of the occurrence of a new phase in the form of inclusions of Al tri- and monohydrates, which generally appear only as a result of treatment in hot (340–373 K) water. In the case of AA obtained in the solution of complex cobalt salt, we observe rather strong absorption both in the above-mentioned regions and in a short-wavelength IR range of 3800–3300 cm^{-1}, which corresponds to stretching vibrations of coordinated and adsorbed OH groups; absorption in the midfrequency region near 1620 cm^{-1}, assigned to Al–OH bending vibrations of Al tri- and monohydrates; and absorption at a frequency of 1080 cm^{-1}, corresponding to stretching vibrations in primary boehmite.

Thus, the phase composition and degree of hydration differ significantly for AA obtained in conventional acid electrolytes and the electrolyte under study ($K_3[Co(C_2O_4)_3]$ solution). In the latter case, AA is characterized by a significant amount of adsorbed and chemically bound moisture and the presence of hydrargillite and boehmite phases, while it hardly contains any unhydrated alumina.

Figure 7 shows X-ray-diffraction spectra of the AA shown in Figs. 6c and 6d. The diffraction patterns, recorded at both sides of the sample, contain five peaks with maxima corresponding to the 2θ values of 38.47°, 44.72°, 65.10°, 78.20°, and 82.31°. These results are in good agreement with the International Centre for Diffraction Data (ICDD) database [58] (files nos. 85-1327 and 89-2769) and the results of study [59]. The intensities of these peaks differ significantly for different sides. The intensities of the X-ray diffraction peaks, corresponding to the metallic aluminum phase, are high for the side oriented oppositely to the cathode during anodic oxiding (Fig. 6d); all four aforementioned peaks can clearly be seen. At the same time, the X-ray-diffraction pattern for the side facing the cathode (Fig. 6c) is significantly different. First, the intensities of the X-ray diffraction peaks corresponding to metallic aluminum decreased to a great extent. Second, one observes two wide peaks with the maxima corresponding to the 2θ values of about 29° and 68°. These peaks are caused by the presence of the AA layer. The same reason (due to X-ray absorption) greatly hinders the occurrence of peaks characteristic of the metallic aluminum phase, which is under a quite thick oxide layer. At the same time, X-ray diffraction from the AA layer can hardly be seen in the curve obtained for the side oriented oppositely to the cathode. This fact is indicative of significantly different thicknesses of the AA film, formed at different anodic

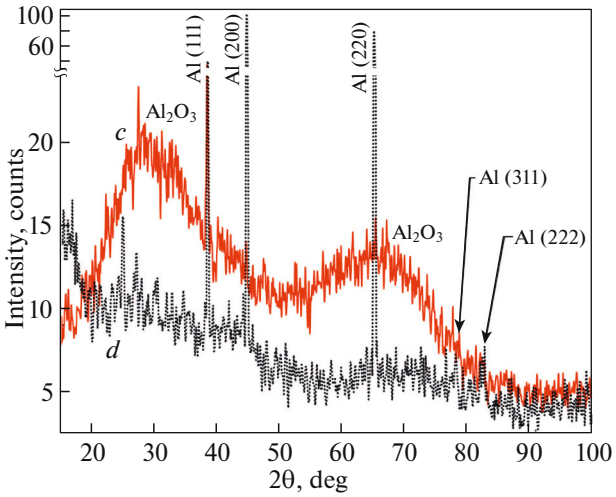

Fig. 7. X-ray-diffraction spectra of the sample obtained in the 1.9 M solution of $K_3[Co(C_2O_4)_3]$ for 29 min at j_a = 1.10×10^2 mA cm^{-2} (solid line *c* and dotted line *d* correspond to the surface faced the cathode (Fig. 6c) and the opposite surface (Fig. 6d), respectively).

sides, which is in good agreement with both the optical images (Figs. 6c, 6d) and the results of IR (Fig. 4f) and PL (Figs. 5b–5f) spectroscopic investigations. The assumption that the wide peaks in the 2θ ranges of 20°–40° and 55°–80° belong to AA is confirmed by analysis of the corresponding ICDD data. X-ray-diffraction spectra of almost any alumina modification contain strong peaks in the above regions (for example, PDF2 database files nos. 31-0026, 46-1215, 04-0876, 08-0013, 09-0440, 52-0803, 71-1125, 79-1559, etc.), which would inevitably undergo significant broadening in a material with a highly disordered structure. At the same time, there have been studies devoted to the structure of porous AA formed in oxalic-acid solutions (the most similar conditions) [60–65] and other electrolytes [20, 63, 64], in which the AA is characterized by a similar X-ray-diffraction pattern typical of an X-ray amorphous material.

Consideration of the X-ray-diffraction spectra presented in Fig. 7 revealed no significant differences from the previously published results, but confirmed once more that the anodic oxiding electrolyte under study is characterized by a low scattering power, the AA formation depends on the anodic surface orientation relative to the cathode, and the thickness of AA formed on the side facing the cathode is larger than that for the opposite side.

CONCLUSIONS

High-purity aluminum was prepared using thermal and mechanical treatments and anodized in the galvanostatic mode at the current densities of (1.5–1.10) × 10^2 and 11.5–30 mA cm^{-2} in aqueous solutions of,

respectively, the K_2[Co(*edta*)] and K_2[Zn(*edta*)] complex compounds with different concentrations. Investigation of the anodic-oxiding processes, morphology, composition, and photoluminescence yielded the following results.

(i) Despite the intense stirring and low anodic current densities, the anodic-oxiding process in K_2[Co(*edta*)] is accompanied by a pronounced "burning" phenomenon, which is characterized by random anodic-voltage oscillations in kinetics.

(ii) The anodic-oxiding kinetics in K_2[Zn(*edta*)] has characteristic periodic oscillations with a large amplitude and regularity, which is indicative of an oscillating electrochemical reaction.

(iii) The anodic-oxiding kinetics in $K_3[Co(C_2O_4)_3]$ has periodic oscillations that are characterized by a higher frequency and a smaller amplitude in comparison with the anodic oxiding in K_2[Zn(*edta*)].

(iv) Protrusions are formed on the surface of the anodic oxide prepared in K_2[Zn(*edta*)] at a low current density (1.5 mA cm^{-2}); they merge into continuous crack fields with an increase in the current density (4.0 mA cm^{-2}). A further increase in j_a (to 10.0 mA cm^{-2}) leads to the formation of "flaky" (or "loose") protrusions, the size and surface density of which increase with a further increase in the current density and anodic-oxiding duration.

(v) Protrusions with a conical and quadrangular-pyramid shape are also formed on the surface of the oxide prepared in $K_3[Co(C_2O_4)_3]$. These protrusions merge into continuous fields with an increase in the current density. The surface density of these protrusions depends on the anodic surface orientation and is always higher for the side facing the cathode. Protrusions formed during aluminum anodic oxiding in $K_3[Co(C_2O_4)_3]$ exhibit no cracking and peeling.

(vi) Auger-electron, electron-probe, and XPS analyses of the AA formed in K_2[Zn(*edta*)] demonstrated the presence of carbon, nitrogen, and sulfur impurities in its composition (the latter was contained in the electrolyte in trace amounts).

(vii) An analysis of the valence state of elements revealed that alumina is present in the α or γ modification; carbon is bound by a nonpolar or weakly polar bond of the C–C, C–H, or C–S type; and sulfur is present in the oxidized state (i.e., it is indeed in the form of sulfate anion).

(viii) An analysis of the photoluminescence spectra of the AA prepared in the K_2[Zn(*edta*)] solution showed that the spectra at the excitation wavelengths of 260 and 340 nm barely differ from those of the samples obtained in conventional acid electrolytes.

(ix) It was established that the photoluminescence spectra of the AA prepared in the $K_3[Co(C_2O_4)_3]$ solutions are characterized by a more complex bell shape and the presence of the second peak, the intensity of which rapidly decreases with an increase in the excitation wavelength. It was found that these specific features are typical of only AA formed on the side facing the cathode and characterized by a large number of protrusions.

(x) It was established that the oxides formed in the K_2[Zn(*edta*)] solution are characterized by high absorption not only in the visible region but also in the IR range under consideration. In the longest-wavelength range (800–400 cm^{-1}, the region of the highest transparency of this sample), the relative transmittance hardly reaches 20%.

(xi) X-ray-diffraction studies showed that the AA sample prepared in the $K_3[Co(C_2O_4)_3]$ solution is an X-ray amorphous material and the thickness of the oxide formed on the anodic side facing the cathode is larger than that for the opposite side.

The performed investigation elucidated some specific features of aluminum anodic oxiding in solutions of chelating complex compounds, morphology, structure, composition, and IR spectroscopic and photoluminescence properties of the anodic alumina films prepared in these electrolytes, marking an important stage in development of the approaches to the formation of anodic alumina with specified composition and electrical and optical characteristics.

ACKNOWLEDGMENTS

We are grateful to the Organizing Committee of the XXV International Symposium "Nanophysics and Nanoelectronics" for the possibility to present the investigation results. We are also grateful to U. Turovets (employee of Belarusian State University of Informatics and Radioelectronics) for the assistance in preparing illustrative material, H. Hildebrand (Friedrich–Alexander-Universität Erlangen–Nürnberg, Germany) for the assistance in carrying out electron-microscopy analyses, S. Lazaruk (Belarusian State University of Informatics and Radioelectronics) for fruitful discussions, and Yu. Radyush (Scientific–Practical Materials Research Center of the National Academy of Sciences of Belarus) for the assistance in performing X-ray diffraction studies.

FUNDING

This study was supported by the State Research Programs of the Republic of Belarus "Convergence-2025" (agreements nos. 3.03.3 and 2.2.6), "Materials Science, New Materials and Technology" (agreement no. 2.02), and "Digital and Space Technologies, Public and State's Security" (agreement no. 1.10.7) and by the Belarussian Republican Foundation for Basic Research and Beijing Institute of Technology (BRFBR–BIT project no. T20PTÈ-006). Part of the investigations were supported by the Deutscher Akademischer Austauschdienst.

CONFLICT OF INTEREST

The authors declare that they have no conflicts of interest.

REFERENCES

1. Y. Lin, G. S. Wu, X. Y. Yuan, T. Xie, and L. D. Zhang, J. Phys.: Condens. Matter **15** (17), 2917 (2003). https://doi.org/10.1088/0953-8984/15/17/339
2. G. Gorokh, A. Mozalev, D. Solovei, V. Khatko, E. Llobet, and X. Correig, Electrochim. Acta **52** (4), 1771 (2006). https://doi.org/10.1016/j.electacta.2006.01.081
3. G. Gorokh, I. Obukhov, A. Poznyak, A. Lozovenko, A. Zakhlebaeva, and E. Sochneva, *Proc. 22nd Int. Crimean Conf. "Microwave & Telecommunication Technology"* (IEEE, Sevastopol, 2012), p. 655.
4. A. N. Pligovka, A. N. Luferov, R. F. Nosik, and A. M. Mozalev, *Proc. 20th Int. Crimean Conf. "Microwave & Telecommunication Technology"* (Sevastopol, 2010), p. 880. https://doi.org/10.1109/CRMICO.2010.5632734
5. W. Lee and S. J. Park, Chem. Rev. **114** (15), 7487 (2014). https://doi.org/10.1021/cr500002z
6. A. Brzózka, A. Brudzisz, K. Hnida, and G. D. Sulka, *Springer Series in Materials Science* (Springer, 2015), Vol. 220, p. 219. https://doi.org/10.1007/978-3-319-20346-1_8
7. A. Santos, J. Mater. Chem. C **5** (23), 5581 (2017). https://doi.org/10.1039/C6TC05555A
8. N. Bogomazova, G. Gorokh, A. Zakhlebayeva, A. Pligovka, A. Murashkevich, and T. Galkovsky, J. Phys.: Conf. Ser. **1124** (8), 081032 (2018). https://doi.org/10.1088/1742-6596/1124/8/081032
9. G. G. Gorokh, I. A. Taratyn, A. N. Pligovka, A. A. Lazavenka, and A. I. Zakhlebayeva, Dokl. Beloruss. Gos. Univ. Inform. Radioelectron. **7** (7), 51 (2019).
10. J. T. Domagalski, E. Xifre-Perez, and L. F. Marsal, Nanomaterials **11** (2), 430 (2021). https://doi.org/10.3390/nano11020430
11. H. Tsuchiya and P. Schmuki, Electrochem. Commun. **7** (1), 49 (2005). https://doi.org/10.1016/J.ELECOM.2004.11.004
12. N. Verma, J. Jindal, K. C. Singh, and A. Mittal, *Advanced Coating Materials* (Wiley, Hoboken, NJ, 2018), p. 235. https://doi.org/10.1002/9781119407652.CH8
13. G. A. Ermolaev, S. E. Kushnir, N. A. Sapoletova, and K. S. Napolskii, Nanomaterials **9** (4), 651 (2019). https://doi.org/10.3390/nano9040651
14. A. I. Sadykov, S. E. Kushnir, N. A. Sapoletova, V. K. Ivanov, and K. S. Napolskii, Scr. Mater. **178**, 13 (2020). https://doi.org/10.1016/j.scriptamat.2019.10.044
15. Yu. Yu. Lur'e, *Handbook of Analytical Chemistry* (Al'yans, Moscow, 2017) [in Russian].
16. S. Tajima, N. Baba, and M. Shimura, Electrochim. Acta **12** (8), 955 (1967). https://doi.org/10.1016/0013-4686(67)80095-1
17. G. C. Wood, P. Skeldon, G. E. Thompson, and K. Shimizu, J. Electrochem. Soc. **143** (1), 74 (1996). https://doi.org/10.1149/1.1836389
18. A. Mozalev, A. Poznyak, I. Mozaleva, and A. W. Hassel, Electrochem. Commun. **3** (6), 299 (2001). https://doi.org/10.1016/S1388-2481(01)00157-6
19. S. K. Lazarouk, D. A. Sasinovich, V. E. Borisenko, A. Muravski, V. Chigrinov, and H. S. Kwok, J. Appl. Phys. **10** (3), 033527 (2010). https://doi.org/10.1063/1.3305672
20. A. Poznyak, A. Pligovka, T. Laryn, and M. Salerno, Materials **14** (4), 767 (2021). https://doi.org/10.3390/ma14040767
21. J. W. Diggle, T. C. Downie, and C. W. Goulding, Chem. Rev. **69** (3), 365 (1969). https://doi.org/10.1021/CR60259A005
22. N. B. Berezin, N. V. Gudin, A. G. Fillipova, V. V. Chevela, Zh. V. Mezhevich, E. D. Yakh'ev, and K. A. Sagdeev, *Electrodeposition of Metals and Alloys from Aqueous Solutions of Complex Compounds* (Kazansk. Gos. Tekhol. Univ., Kazan', 2006) [in Russian].
23. V. V. Zenin, A. A. Stoyanov, S. V. Petrov, and B. A. Spiridonov, Russ. Microelectron. **42** (5), 288 (2013). https://doi.org/10.1134/S1063739713040082
24. L. de Riese-Meyer and V. Sander, Aluminium **1** (2), 155 (1992).
25. V. F. Surganov and A. A. Poznyak, Russ. J. Appl. Chem. **71** (2), 253 (1998).
26. A. Mozalev, I. Mozaleva, M. Sakairi, and H. Takahashi, Electrochim. Acta **50** (25–26), 5065 (2005). https://doi.org/10.1016/J.ELECTACTA.2005.02.092
27. I. Kleschenko, M. Rezvanova, and A. Poznyak, *Proc. 16th Int. Crimean "Microwave and Telecommunication Technology"* (Sevastopol, 2006), p. 675. https://doi.org/10.1109/CRMICO.2006.256153
28. T. Lednický and A. Mozalev, *Proc. 7th Int. Conf. on Nanomaterials – Research & Application* (Brno, Czech Republic, October 14–16, 2015), p. 265.
29. A. A. Poznyak, *Abstr. Int. Sci.-Tech. Conf. "Electrochemical and Electrolyte-Plasma Methods of Modification of Metal Surfaces"* (Kostromsk. Gos. Univ., Kostroma, 2003), p. 38.
30. S. V. Golovataya, O. I. Zubarevich, G. Knörnschild, E. V. Muravitskaya, and A. A. Poznyak, *Proc. 11th Int. Sci.-Tech. Conf. "Modern Means of Communication"* (Bestprint, Minsk, 2006), p. 72.
31. S. V. Golovataya, O. I. Zubarevich, G. Knörnschild, and A. A. Poznyak, *Proc. 12th Int. Sci.-Tech. Conf. "Modern Means of Communication"* (VGKS, Minsk, 2007), p. 68.
32. S. V. Golovataya, O. I. Zubarevich, G. Knörnschild, E. V. Muravitskaya, and A. A. Poznyak, *Proc. 18th Int. Crimean Conf. "Microwave and Telecommunication Technology"* (Sevastopol, 2008), p. 581. https://doi.org/10.1109/CRMICO.2008.4676512
33. S. V. Golovataya, N. V. Koval'chuk, and A. A. Poznyak, *Proc. 14th Int. Sci.-Tech. Conf. "Modern Means of Communication"* (VGKS, Minsk, 2009), p. 102.
34. S. V. Golovataya, A. G. Karoza, N. V. Koval'chuk, and A. A. Poznyak, *Proc. 14th Int. Sci.-Tech. Conf. "Modern*

Means of Communication" (VGKS, Minsk, 2007), p. 104.

35. A. A. Poznyak, G. Knörnschild, and A. G. Karoza, *Proc. 21st Int. Crimean Conf. "Microwave and Telecommunication Technology"* (IEEE, Sevastopol, 2011), p. 723.

36. S. V. Golovataya, A. M. Mozalev, and A. A. Poznyak, *Proc. 16th Int. Crimean Conf. "Microwave and Telecommunication Technology" (CriMiCo)* (Sevastopol, 2006), p. 606. https://doi.org/10.1109/CRMICO.2006.256125

37. A. M. Mozalev, I. I. Mozaleva, and A. A. Poznyak, Dokl. Beloruss. Gos. Univ. Inform. Radioelectron. **2** (14), 127 (2006).

38. G. Knörnschild, A. A. Poznyak, A. G. Karoza, and A. Mozalev, Surf. Coat. Technol. **275**, 17 (2015). https://doi.org/10.1016/J.SURFCOAT.2015.04.030

39. A. A. Poznyak, *Anodic Aluminum Oxide and Composite Materials Based on It: Monograph* (Izd. Tsentr Beloruss. Gos. Univ., Minsk, 2007) [in Russian].

40. G. G. Gorokh, A. M. Mozalev, and A. A. Poznyak, *Proc. 9th Conf. of Young Scientists and Specialists* (Novosibirsk, 1988), Vol. 1 (2), p. 9.

41. A. A. Poznyak, G. Knörnschild, and M. Stratmann, *Proc. 5th All-Russian Sci.-Tech. Conf. "Actual Problems of Solid-State Electronics and Microelectronics"* (Taganrogsk. Gos. Radiotekn. Univ., Taganrog, 1998), p. 38.

42. W. J. Stępniowski, M. Norek, M. Michalska-Domańska, A. Nowak-Stępniowska, A. Bombalska, M. Włodarski, and Z. Bojar, Mater. Lett. **106**, 242 (2016). https://doi.org/10.1016/J.MATLET.2013.05.016

43. A. I. Kosevich, "Dislocation," in *Physical Encyclopedia* (Sov. Entsiklopedia, Moscow, 1988), Vol. 1, p. 636 [in Russian].

44. V. V. Boldyrev, "Defects," in *Chemical Encyclopedia* (Sov. Entsiklopedia, Moscow, 1990), Vol. 2, p. 29 [in Russian].

45. T. H. Nguyen and R. T. Foley, J. Electrochem. Soc. **126** (11), 1855 (1979). https://doi.org/10.1149/1.2128815

46. C. B. Bargeron and R. B. Givens, J. Electrochem. Soc. **124** (8), 1230 (1977). https://doi.org/10.1149/1.2133533

47. A. M. Zhabotinskii, "Oscillatory reactions," in *Chemical Encyclopedia* (Sov. Entsiklopedia, Moscow, 1990), Vol. 2, pp. 428–430 [in Russian].

48. V. V. Nechiporuk and I. L. El'gurt, *Self-Organization in Electrochemical Systems* (Nauka, Moscow, 1992) [in Russian].

49. S. Ono, M. Saito, M. Ishiguro, and H. Asoh, J. Electrochem. Soc. **151** (8), B473 (2004). https://doi.org/10.1149/1.1767838

50. T. Aerts, I. De Graeve, and H. Terryn, Electrochim. Acta **54** (2), 270 (2008). https://doi.org/10.1016/J.ELECTACTA.2008.08.004

51. F. Zhou, A. K. Mohamed Al-Zenati, A. Baron-Wiecheć, M. Curioni, S. J. Garcia-Vergara, H. Habazaki, P. Skeldon, and G. E. Thompson, J. Electrochem. Soc. **158** (6), C202 (2011). https://doi.org/10.1149/1.3578028

52. N. M. Yakovleva, A. M. Shul'ga, K. V. Stepanova, A. N. Kokatev, V. S. Rudnev, I. V. Lukiyanchuk, and V. G. Kuryavyi, Kondens. Sredy Mezhfaz. Granitsy **22** (1), 124 (2020). https://doi.org/10.17308/kcmf.2020.22/2536

53. K. V. Stepanova, A. M. Shul'ga, N. M. Yakovleva, and A.N. Kokatev, Tr. Kol'sk. Nauchn. Tsentra Ross. Akad. Nauk **11** (3), 185 (2020). https://doi.org/10.37614/2307-5252.2020.3.4.040

54. T. A. Carlson, *Photoelectron and Auger Spectroscopy* (Springer, Boston, 1975). https://doi.org/10.1063/1.3023614

55. E. Hornbogen and B. Skrotzki, *Werkstoff-Mikroskopie* (Springer, Berlin–Heidelberg, 1993), Vol. 11.

56. R. I. Agladze, N. G. Gofman, N. T. Kudryavtsev, L. L. Kuz'min, and A. P. Tomilov, *Applied Electrochemistry: Manual*, Ed. by N. T. Kudryavtseva (Khimiya, Moscow, 1975) [in Russian].

57. G. G. Gorokh, Candidate's Dissertation in Engineering (Minsk Radiotech. Inst., Minsk, 1989).

58. ICDD – International Centre for Diffraction Data. https://www.icdd.com/. Accessed April 4, 2021.

59. T. Lebyedyeva, S. Kryvyi, P. Lytvyn, M. Skoryk, and P. Shpylovyy, Nanoscale Res. Lett. **11** (1), 203 (2016). https://doi.org/10.1186/s11671-016-1412-y

60. L. Zhou, Y. Guo, M. Yagi, M. Sakurai, and H. Kameyama, Int. J. Hydrogen Energy **34** (2), 844 (2009). https://doi.org/10.1016/J.IJHYDENE.2008.10.057

61. T. Masuda, H. Asoh, S. Haraguchi, and S. Ono, Electrochemistry **82** (6), 448 (2014). https://doi.org/10.5796/ELECTROCHEMISTRY.82.448

62. T. Masuda, H. Asoh, S. Haraguchi, and S. Ono, Materials (Basel) **8** (3), 1350 (2015). https://doi.org/10.3390/ma8031350

63. S. M. Suchitra, P. R. Reddy, and N. K. Udayashankar, AIP Conf. Proc. **1728** (2), 020407 (2016). https://doi.org/10.1063/1.4946458

64. P. R. Reddy, K. M. Ajith, and N. K. Udayashankar, Appl. Phys. A **124** (11), 765 (2018). https://doi.org/10.1007/S00339-018-2163-7

65. P. R. Reddy, K. M. Ajith, and N. K. Udayashankar, Mater. Sci. Semicond. Process. **106**, 104755 (2020). https://doi.org/10.1016/j.mssp.2019.104755

Translated by A. Sin'kov